System-Wide Hierarchical Coupling of Brain and Body Rhythms Under State and Latent Stress

Asa Young[1]*, Jonathan Roberts[1], Stephen Baumgart[1], Marissa Ericson[2], Alan Macy[3], Justin Riddle[4], Jonathan W. Schooler[1]

[1]Department of Psychological and Brain Sciences, University of California Santa Barbara, Santa Barbara, California, USA

[2]Biostatistics, Epidemiology and Research Design (BERD), University of California, Irvine, Orange, California, USA

[3]BIOPAC Systems, Inc, Goleta, California, USA

[4]Department of Psychology, Florida State University, Tallahassee, Florida, USA

Correspondence should be addressed to:

Asa Young

asayoung@ucsb.edu

Abstract

The present study assessed *harmonic locking*, the coordination of frequency that enables cross-frequency phase synchrony, between the EEG, heart rate, and breathing frequency. In two state-based experiments, harmonic locking emerged as a system-wide property of brain-body coordination, associated with cognitive demand, task-related physiological arousal, and negative affect valence. Cardiorespiratory rhythms coupled to low-frequency, network-level brain rhythms, which in turn coupled to higher-frequency brain activity, enabled by a coordinated, oppositional modulation of low- and high-frequency rhythms. The converging effects of cognitive demand, physiological arousal, and negatively-valenced affect suggest a conceptual and functional overlap, potentially unified as constituent elements of state stress. A third, meta-analytical experiment found individual differences in perceived stress and interoceptive sensitivity to physiological arousal predicted latent expression of brain-body coupling. Finally, distinct elements of the stress response engaged distinct modes of synchrony, contingent on arousal activation: a purely cognitive stress promoted theta-anchored intra-brain coupling; stress accompanied by cardiorespiratory activation promoted delta-anchored brain-body coupling. Together, this study identified harmonic locking as a stress-responsive, hierarchically-organized substrate of brain-body coordination.

I. Introduction

The heart beats, the lungs breathe, and the brain waves. An organism can be described as a collection of fast and slow rhythms, coordinated to maintain its health and produce its behavior. An intriguing conjecture is that these rhythms are not isolated, but form an integrated hierarchy where brain and bodily rhythms are organized in a scale-invariant manner (Klimesch, 2013; 2018). This perspective aligns with the emerging view that cognitive neuroscientific research can be simplified from a near-infinite information space to a set of constrained trajectories that are determined by the brain's interactions with its internal and external environment (Kluger et al. 2024). Here, we investigate how the coordination of brain and body rhythms fluctuates with task demands, affective state, and individual differences.

A rhythm can be analyzed through three dimensions: frequency (cycling rate), amplitude or power (magnitude of the signal), and phase (position within the cycle). Brain activity can be characterized, broadly, by five putative, evolutionarily-stable rhythms varying in frequency each of which possess idiosyncratic characteristics to their waveforms and associated cognitive functions (Fields, 2020). The spatial distribution of each rhythm is constrained by the physics of wave propagation: with increasing frequency, signals become less coherent over distance (Dehaene, 2014). Hence, frequency defines a spatiotemporal hierarchy wherein a

given cognitive process may be propagated across a large-scale network or confined to local –albeit higher-frequency– cortical processing (Canolty & Knight, 2010). Cross-frequency coupling (CFC) defines a category of interaction that enables coordination between rhythms of varying timescales such as between low- and high-frequency brain activity or between bodily rhythms and the brain (Canolty & Knight, 2010; Klimesch, 2018). Through a coordination of fast and slow rhythms, the system is able to effectively unify in time the activity of distributed systems varying in informational content, complexity, and function (Hyafil et al., 2015).

CFC can manifest as any combination of frequency, amplitude, or phase, but the most extensively studied and functionally relevant forms are phase-phase coupling between low- and high-frequency phases (Lachaux et al., 1999), and phase-amplitude coupling in which the phase of a low-frequency rhythm modulates the amplitude of a higher-frequency rhythm (Yakubov et al. 2022). The present study focused on phase-phase coupling, motivated by a recent theory proposing that the frequency bands characterizing brain and cardiorespiratory activity are uniquely structured to promote this form of cross-frequency coordination (Klimesch, 2013; 2018). Two rhythms can coordinate their excitatory phases by maintaining a constant phase difference over time, which is most stable when the two rhythms achieve a harmonic or integer ratio between their frequencies (e.g. r = fast/slow = harmonic; Palva & Palva, 2018). This principle is reflected latently in the center frequencies of the putative brain and

cardiorespiratory rhythms. Gamma (40 Hz), beta (20 Hz), alpha (10 Hz), theta (5 Hz), and delta (2.5 Hz) bands are related in integer multiples. Typical resting heart rate is 1.25 Hz, aligning with delta, and the preferred breathing frequencies (0.3125, 0.1562, and 0.0781 Hz) are integer subdivisions of the heart rate. As such, the rhythmic architecture of the brain and cardiorespiratory system provides an intrinsic substrate for cross-frequency coordination within and between systems.

Frequency is nonstationary and may transiently accelerate or decelerate according to internal states and external demands (Cohen, 2014; Samaha et al., 2015). Consequently, CFC can vary with state-related factors. The coupling of two frequencies in harmonic ratios, hereafter referred to as *harmonic locking*, is modulated by physiological arousal and cognitive demand. For example, harmonic locking between alpha, heart rate, and breathing frequency is enhanced during wakefulness relative to sleep (Rassi et al., 2019). Alpha-theta harmonic locking increases linearly from meditative to mind wandering to cognitively demanding states (Rodriguez-Larios et al., 2019, 2020, 2021), and alpha-heart rate harmonic locking is greater in cognitive tasks compared to meditation (Soriano et al., 2024). Together, these findings suggest harmonic locking, as tested in a limited array of brain and bodily rhythms, is associated with transitions from low- to high-demand states.

Harmonic locking may vary as a function of trait-related factors. Individuals with autism exhibit greater harmonic locking of alpha and theta

rhythms at rest relative to control cohorts (Alaerts et al., 2024). This coupling decreases following the administration of intranasal oxytocin (Alaerts et al., 2021, 2024), a neuromodulator with anxiolytic effects. In both neurotypical and autistic cohorts, alpha-theta harmonic locking is negatively associated with low-frequency HRV and positively associated with high-frequency HRV. This would suggest that enhanced harmonic locking may be associated with increased subjective distress, though this too was tested in a narrow range of brain rhythms.

Although harmonic locking as a form of cross-frequency coordination appears to index cognitive demand, physiological arousal, and subjective distress, the evidence has emerged from a limited arrangement of brain and bodily rhythms. However, as noted, theoretical accounts of frequency architecture posit that brain and cardiorespiratory rhythms are organized in a scale-invariant manner, such that any pair of rhythms can, in principle, achieve harmonic locking, thereby enabling the functional coordination of brain and body as a unified system (Klimesch, 2018). The present article addressed this gap by examining state- and trait-related fluctuations in harmonic locking across all configurations of brain and cardiorespiratory rhythms. Accordingly, we predicted that harmonic locking generalizes beyond specific rhythm pairs to a system-wide property of brain-body coordination. Experiment 1 (n = 23) tested the modulation of harmonic locking by cognitive demand, Experiment 2 (n = 37) examined its sensitivity to affective valence, and a third, meta-analytical study (n = 60) pooled

across both datasets to identify demographic predictors of brain-body coupling.

II. Experiment 1

Methods

Experimental Design

Experiment 1 was inspired by Rodriguez-Larios and colleagues (2020; 2021), who demonstrated that harmonic locking between the alpha and theta bands was modulated by cognitive demand. Participants completed three within-subjects conditions –a meditative task, a resting state, and an arithmetic task– designed to provide a continuous contrast of active cognitive processing (meditation < rest < arithmetic). This gradient is supported by prior findings showing enhanced harmonic locking between executive and memory systems during 1) cognitive tasks relative to mind wandering and meditation (arithmetic > mind wandering & meditation; Rodriguez-Larios et al., 2019; 2020), and 2) mind wandering relative to meditation (mind wandering > meditation; Rodriguez-Larios et al., 2021).

The present study adopted the three-condition, within-subjects design described above and expanded the list of tested rhythm pairs beyond alpha and theta (see section Harmonic Locking Calculation). In the meditative condition, participants performed a resonant breathing task, a common

component of contemplative practices (Shaffer et al., 2014), by synchronizing their breathing to a repeating 10-second timer (0.1 Hz) or as close to 10-second cycles as was achievable for 12 minutes. The rest (or mind wandering) condition instructed participants to remain relaxed and engage in undirected thought for 15 minutes. A fixation cross was provided. The arithmetic task involved the iterative subtraction of 7's from 1000 (e.g. 1000, 993, 986…) in four-, five-, and three-minute trials, in that order, after which they reported what number they were presently on. Participants were instructed to restart from 1000 if they reached zero or lost their way. All three conditions were "eyes-open" recordings and were completed in a random order. The study was approved by the Institutional Review Board of the University of California, Santa Barbara.

Participants

27 healthy, neurotypical individuals were recruited from the student population for a single-session study conducted in the Memory Emotion Thought Awareness (META) Laboratory at the University of California, Santa Barbara. Eligibility criteria excluded individuals with a history of cardiorespiratory, gastrointestinal, or neuropsychiatric disorders, as well as traumatic brain injury. Data from four participants were excluded due to incomplete participation, yielding a sample of 23 participants (12 female; mean age = 24.48 years; mean BMI = 24.31 kg/m^2).

Data Collection

EEG was recorded using a standard 19-channel Electro-Cap International cap (10-20 system) and sampled at 1,000 Hz with a TMSi Mobita wireless amplifier. Cardiorespiratory signals were acquired in parallel at 1,000 Hz with a BIOPAC MP160 system equipped with two modules for electrocardiography (ECG100C) and respiratory effort (RSP100C). ECG was captured using two BIOPAC EL503 electrodes placed on either side of the left chest cavity and one EL503 electrode placed on the right rib cage as a ground. Respiratory effort was assessed via a TSD201 transducer that detects abdominal circumference changes during respiration. BIOPAC Systems Acqknowledge 5.0 data acquisition and analysis software was employed for signal acquisition in both amplifiers.

To achieve temporal alignment, both amplifiers monitored a light-sensitive diode affixed to the participant's screen. Black-white flashes were presented to the diode, hidden from the participant, to mark the start and end of each condition and, additionally, every 10 seconds to correct for drift between amplifiers. These pulses were used to align and epoch the EEG and cardiorespiratory signals using in-house MATLAB scripts during preprocessing.

Data Pre-Processing

Data was exported from Acqknowledge 5.0 as MATLAB (2023a) files. EEG recordings were imported into EEGLAB (Delorme & Makeig, 2004) for

preprocessing. Raw data was bandpass filtered 0.5-50 Hz, excluding the light-sensitive channel. Signals were re-referenced to the average, after which channel data and power spectra were inspected to identify dead or noisy electrodes. Bad channels were removed prior to independent component analysis (ICA). ICA components were automatically classified using ICLabel (Pion-Tonachini et al., 2019) and inspected visually to reject noise components. Rejected channels were interpolated after component rejection.

Artifacts were identified using a 10-second Hanning window with 50% overlap. Windows exceeding ±50 µV were marked as artifacts and removed, along with their corresponding cardiorespiratory epochs. To minimize the contribution of the aperiodic component of the EEG (the background 1/f activity), each window was detrended by fitting its slope with a robust linear regression (excluding the alpha range) and subtracting this slope from the short-term fast Fourier transform (FFT). Residual oscillatory peaks surviving aperiodic attenuation were detected using find-local-maxima functions[1]. If a peak fell within the canonical frequency ranges –delta (1-4 Hz), theta (4-8 Hz), alpha (8-14 Hz), beta (14-30 Hz), or gamma (30-50 Hz)– the window was filtered to that band using a plateau-shaped, zero-phase filter with 15% transition zones and the appropriate cutoff frequencies.

1 This method was modeled after Rodriguez-Larios et al (2019) whose processing code was shared publicly on the Open Science Framework (OSF) and was of great help in our own processing.

Instantaneous frequency time series were estimated by multiplying the first temporal derivative of the angle of the Hilbert transform by the sampling rate and dividing by 2π. To attenuate spurious noise-driven spikes in the frequency time series, a median filter of 10 steps between 10 and 400 milliseconds was applied, which reassigns each sample to the median of a distribution of medians of surrounding samples. If a frequency band's oscillation did not survive aperiodic attenuation, it was dummy-coded as such and those timepoints excluded from further analyses. The filtering, frequency estimation[2], and median filtering were implemented in accordance with Cohen (2014).

Cardiorespiratory signals were preprocessed separately. Respiratory effort was band-pass filtered between 0.01 and 20 Hz using a second-order Butterworth filter. Breathing instantaneous frequency was estimated using the same procedure applied to the EEG bands. Given the non-sinusoidal nature of cardiac activity, heart rate was derived from the ECG using an AcqKnowledge 5.0 calculation channel, which transformed the raw signal into a beats-per-minute (BPM) time series at the original sampling rate, later converted to Hz. To ensure temporal alignment with the EEG, heart rate and respiration frequency time series were segmented using the same overlapping window procedure. The resulting EEG and cardiorespiratory frequency time series were then concatenated for analysis.

---

2 The MATLAB syntax for estimating instantaneous frequency employed in the present study, courtesy of Cohen (2014): srate*diff(unwrap(phaseangles))/(2*pi)

Harmonic Locking Calculation

To quantify cross-frequency coordination within and between the brain and cardiorespiratory system, instantaneous frequency ratios were computed for all pairwise combinations of higher- and lower-frequency signals (e.g., alpha/theta, alpha/delta, alpha/heart rate). Ratios were obtained by element-wise division of the instantaneous frequency time series, and harmonic locking was defined as the incidence (proportion of time points) at which these ratios fell within ±0.05 of the appropriate integer value. Theoretical accounts of frequency architecture posit a doubling/halving rule of organization such that, for example, alpha (f_1 = 10 Hz) may couple with theta (f_2 = 5 Hz) at a 2:1 ratio or with delta (f_3 = 2.5 Hz) at a 4:1 ratio (Klimesch, 2013, 2018). For each high-low frequency pairing, the harmonic was selected according to this doubling/halving rule (see Fig. 5 of Klimesch, 2018). For frequency pairings that included breathing frequency, harmonic locking was pooled across breathing frequency modes.

Statistical Analysis

To test the linear effect of cognitive demand on harmonic locking, condition was modeled as an ordinal predictor (meditation < rest < arithmetic) within a mixed-effects model, such that each unit increase represented an increase in condition-related cognitive demand, consistent with Rodriguez-Larios et al. (2020). The effect of participants' breathing

frequency was likewise tested as a continuous predictor within a mixed-effects model, given that it was experimentally constrained during the meditative condition and fluctuates as a function of task-related arousal.

To control for inflated Type I error due to multiple comparisons, we employed a cluster-based permutation procedure (Maris & Oostenveld, 2007). Test statistics were computed at each channel, thresholded, and grouped into clusters of spatially adjacent electrodes[3] showing statistically significant effects of the same sign. Data were then permuted 1,000 times at the electrode level, and the clustering procedure repeated to generate a null distribution of maximum cluster sizes. Empirical cluster sizes exceeding the threshold of this null distribution were deemed statistically significant.

The dataset was high-dimensional, so the analysis was approached in two stages. In the first stage, we tested for system-wide patterns of harmonic locking across the brain and cardiorespiratory system. Two-tailed mixed-effects models were fitted at each channel, collapsing across EEG-EEG and EEG-cardiorespiratory rhythm pairings (with pairing labels included as covariates)[4]. This yielded a single test statistic at each channel representing the effect of the predictor variable on global harmonic locking, which was then submitted to permutation testing and cluster-based correction. In the second stage, if a global effect was observed, one-tailed

---

3 The adjacency matrix was generated using the ft_prepare_neighbours function from the FieldTrip toolbox (Oostenveld et al., 2011).

4 The linear regression formula was structured like so:

> Harmonic Incidence ~ Predictor (cognitive demand or breathing frequency) + Rhythm Pair Label (categorical covariate) + Condition Length + (Predictor's Random Slope | Participant ID)

models were conducted separately for each rhythm pairing to test directional hypotheses[5]. To correct for the multiple comparisons arising from multiple cluster-based permutation models testing each rhythm pair, the alpha value for determining a significant cluster was adjusted to $\alpha = 0.0025$ ($\alpha = 0.05 / 20$ models). Given the volume of topographical plots generated in this stage, we report only those rhythm pairs with significant clusters. The topographical plots and cluster statistics for all rhythm pairs are provided in the Supplementary Materials.

Non-spatialized datasets such as the heart-breath harmonic locking and cardiorespiratory frequency modulation were assessed with the mixed-effects models described above without further correction.

Secondary Analyses

Two additional analyses were conducted to characterize the specificity of cross-frequency interactions and the frequency modulation underlying harmonic locking. First, to test whether observed effects were confined to the harmonic or reflected a broader, non-specific pattern across the ratio spectrum, we estimated the incidence of all possible ratios for each rhythm pair. For each pairing, a ratio range and step size were defined (see Supplementary Table 1), and instantaneous frequency ratios were rounded to the nearest step value. Incidence was then computed as the

---

5 The linear regression formula was structured like so:
Harmonic Incidence ~ Predictor (cognitive demand or breathing frequency) + Condition Length + (Predictor's Random Slope | Participant ID)

proportion of samples assigned to each ratio value, and mixed-effects models were applied to test predictor effects across the full ratio spectrum.

Second, to assess whether cross-frequency effects could be attributed to systematic shifts in EEG band frequencies, a parallel analysis was conducted at the level of individual EEG bands. A range of possible values was generated between each EEG band's high and low pass cutoffs in 0.1 Hz step sizes. The incidence of each frequency within the frequency band was estimated and submitted to the mixed-effects models. As described in subsequent discussions, an increase in the incidence of higher-frequency values within a frequency band relative to its lower-frequency values will be referred to as an *acceleration* and the opposite will be referred to as a *deceleration*. Both secondary analyses are presented within the Supplementary Materials, though the latter is referenced within the text.

Results and Discussion

Cardiorespiratory Frequency Modulation & Heart-Breath Harmonic Locking

Mixed-effects models tested the effect of cognitive demand on average heart rate and breathing frequency. Cognitive demand accelerated heart rate [$\beta = 0.013$, $t(40.534) = 2.138$, $p = 0.039$] and breathing frequency [$\beta = 0.074$, $t(25.586) = 11.707$, $p < 0.001$]. As breathing frequency was experimentally manipulated in the meditative condition, it was re-assessed

using one-way repeated-measures ANOVA. Consistent with the linear regression, a significant effect of condition was found, $F(2, 44) = 87.36$, $p < .001$, generalized $\eta^2 = .66$. Pairwise comparisons with Bonferroni correction indicated that respiration was significantly faster during arithmetic ($M = 0.22$, $SE = 0.01$) than both rest [$M = 0.17$, $SE = 0.01$; $t(22) = -6.02$, $p < .001$] and meditation conditions [$M = 0.07$, $SE = 0.004$; $t(22) = -13.22$, $p < .001$], and faster during rest than meditation [$t(22) = 7.02$, $p < .001$].

An identical model tested the effect of cognitive demand on harmonic locking between heart rate and breathing frequency. Heart-breath harmonic locking was enhanced by cognitive demand [$\beta = 0.865$, $t(24.595) = 10.089$, $p < 0.001$]. A separate model, replacing cognitive demand with breathing frequency, indicated an enhancement of heart-breath harmonic locking as breathing frequency accelerated [$\beta = 11.898$, $t(50.218) = 18.046$, $p < 0.001$]. Including both cognitive demand [$\beta = 0.226$, $t(61.537) = 2.079$, $p = 0.042$] and breathing frequency [$\beta = 8.672$, $t(64.732) = 6.888$, $p < 0.001$] within the mixed-effects model raised the possibility of a mediation model discussed and tested in the Supplementary Materials (Supplementary Fig. 7).

Harmonic Locking is Enhanced by Cognitive Demand

The linear regression identified a significant, positive cluster involving all EEG channels, $t_{cluster}(1358) = 56.599$, $p < 0.001$. Harmonic locking increased linearly from meditation to resting state to arithmetic tasks in

EEG-EEG and EEG-cardiorespiratory rhythm pairings. Although the cluster spanned the scalp, the topographical distribution of fixed-effect t-values (Fig. 1) suggested that the effect was strongest over frontal (F3, Fz, F4) and posterior (O1, O2, Pz) cortices, linked to executive and visual processing, respectively. These results, with the finding that cognitive demand enhanced heart-breath harmonic locking, indicate that harmonic locking is a system-wide phenomenon for coordinating brain and cardiorespiratory rhythms, indexing transitions from low- to high-demand states.

The analysis of each rhythm pairing revealed four central findings. First, the coupling of EEG to breathing frequency is thoroughly enhanced by cognitive demand (Fig. 2D & 2G). Linear models assessing gamma- [$t_{cluster}(66) = 210.567$, $p < 0.001$], beta- [$t_{cluster}(66) = 200.419$, $p < 0.001$], alpha- [$t_{cluster}(66) = 187.213$, $p < 0.001$], theta- [$t_{cluster}(66) = 215.027$, $p < 0.001$], and delta-breath harmonic locking [$t_{cluster}(66) = 208.339$, $p < 0.001$] identified significant, positive clusters comprising all EEG channels. Second, the modulation of EEG-heart coupling involved the low-frequency, network-level rhythms (Fig. 2C & 2H). Significant, positive clusters were identified for delta-heart coupling involving the majority of EEG channels [$t_{cluster}(66) = 36.375$, $p < 0.001$] and theta-heart coupling comprising frontal and central channels [$t_{cluster}(66) = 14.129$, $p < 0.001$]. Third, cognitive demand enhanced the coupling of low-frequency, network-level brain rhythms to comparatively higher-frequency EEG (Fig. 2B & 2E). Significant, positive clusters were identified for harmonic locking between theta and delta

involving frontal and midline channels [$t_{cluster}(66) = 21.758$, $p < 0.001$]; alpha and delta in frontal channels [$t_{cluster}(66) = 11.778$, $p < 0.001$]; beta and delta comprising the majority of channels [$t_{cluster}(66) = 30.078$, $p < 0.001$]; and gamma and theta also comprising the majority of channels [$t_{cluster}(66) = 23.586$, $p < 0.001$]. Lastly, coupling among higher-frequency EEG bands was enhanced by cognitive demand (Fig. 2A & 2F). Significant, positive clusters were detected for gamma-beta [$t_{cluster}(66) = 47.582$, $p < 0.001$] and gamma-alpha coupling [$t_{cluster}(66) = 28.023$, $p < 0.001$] involving the majority of channels.

There was an emergent pattern that suggested a hierarchical organization of EEG and cardiorespiratory rhythms. As a function of cognitive demand, delta –a low-frequency, network-level rhythm commonly associated with executive function and top-down control (Helfrich et al., 2017; Riddle et al., 2021)– synchronized to both cardiorespiratory rhythms and higher-frequency EEG. The motivating theory behind the present study, the binary hierarchy brain body oscillation theory (Klimesch, 2018), proposed that brain and body rhythms are latently aligned in a nested, hierarchical fashion and that this mode of organization is enhanced in a task-relevant manner. Earlier accounts, such as the oscillatory hierarchy hypothesis (Lakatos et al., 2005), proposed that low-frequency brain rhythms entrain to rhythmic stimuli and modulate higher-frequency activity, enabling nested components to synchronize with stimuli of interest. The present findings suggest the hierarchical principle extends to frequency

alignment, whereby high-frequency EEG is nested within low-frequency EEG, and low-frequency EEG is uniquely suitable for coupling with bodily signals.

Analysis of frequency indicated delta accelerated, while theta, alpha, and beta decelerated, with gamma occupying a middle ground position within its spectrum (Supplementary Fig. 3). Both heart rate and breathing frequency accelerated with task demands. These results suggest that the majority of rhythm pairs whose coupling was enhanced by cognitive demand were driven by the acceleration of lower-frequency rhythms and the deceleration of comparatively higher-frequency rhythms.

The analysis of harmonic locking within and between brain and cardiorespiratory rhythms yielded three converging findings. First, harmonic locking increased with cognitive demand in a scale-invariant manner, encompassing EEG-EEG, EEG-cardiorespiratory, and heart-breath coupling, with emphasis over frontal and posterior cortices. Second, the pattern of enhanced coupling pointed to a hierarchical organization in which cardiorespiratory rhythms coupled to low-frequency EEG, and these low-frequency rhythms in turn coupled to higher-frequency brain activity. Third, this was driven by the oppositional acceleration of lower-frequency rhythms and deceleration of higher-frequency rhythms.

Harmonic Locking is Enhanced by Accelerated Breathing Frequency

Breathing frequency increased systematically with cognitive demand. Following prior work (Grassmann et al., 2016), this acceleration can be interpreted as a proxy for task-related arousal. Accordingly, we conducted additional linear models using each participant's average breathing frequency per condition as an index of arousal, testing how task-related arousal modulated harmonic locking.

A significant, positive cluster was identified involving the majority of EEG channels [$t_{cluster}(1358) = 39.677$, $p < 0.001$]. As breathing frequency accelerated system-wide harmonic locking was enhanced. The topographical distribution of fixed-effect t-values closely resembled the effect of cognitive demand, with frontal and posterior foci (Fig. 3), although less extensively[6]. These results, with the finding that accelerated breathing enhanced heart-breath coupling, indicate that system-wide harmonic locking within and between the brain and cardiorespiratory system is sensitive to indices of physiological arousal.

The linear models conducted for each rhythm pair yielded similar results. First, as breathing frequency increased, coupling of gamma

---

6 One plausible reason for this discrepancy, despite the correlation between cognitive demand and breathing frequency, is evident in the electrode-level plots when presented with a *loess* line instead of an *lm* line: the relationship between breathing frequency and harmonic locking was not strictly linear but appeared quadratic –an inverted-U– such that harmonic locking increased with acceleration up to ~0.1 Hz beyond one's resting breathing frequency, after which further acceleration reduced coupling. The Yerkes-Dodson-style observation though is anecdotal; testing for a quadratic relationship in Fz and Pz did not improve model fit (Fz: AIC = 3212.1 vs. 3215.0, BIC = 3342.8 vs. 3340.5, $\chi^2(1) = 0.10$, $p = .76$; Pz: AIC = 3637.4 vs. 3642.7, BIC = 3768.2 vs. 3768.3, $\chi^2(1) = 2.23$, $p = .14$). The present study did not include a condition that elicited strong arousal, resulting in sparse data points beyond +0.1 Hz from one's resting-state breathing frequency. Future work incorporating manipulations such as moderate exercise or high-difficulty cognitive tasks (e.g. 3-back) may be better positioned to capture the upper range of the inverted-U relationship.

[$t_{cluster}(66) = 358.835$, $p < 0.001$], beta [$t_{cluster}(66) = 467.497$, $p < 0.001$], alpha [$t_{cluster}(66) = 492.745$, $p < 0.001$], theta [$t_{cluster}(66) = 1049.030$, $p < 0.001$], and delta [$t_{cluster}(66) = 274.633$, $p < 0.001$] to breathing frequency was significantly enhanced scalp-wide (Fig. 4D & 4G). Second, modulation of EEG-heart coupling was more restricted (Fig. 4C & 4H), with only delta-heart coupling showing a significant positive cluster involving the majority of channels [$t_{cluster}(66) = 29.634$, $p < 0.001$]. Third, the modulation of low- to high-frequency EEG coupling was limited to the frontal cortex (Fig. 4B). Significant positive clusters were identified for theta-delta coupling [$t_{cluster}(66) = 12.942$, $p < 0.001$] and beta-delta coupling in frontal and midline channels [$t_{cluster}(66) = 23.413$, $p < 0.001$]. Last, higher-frequency EEG coupling showed enhancement with accelerated breathing (Fig. 4A & 4F). Significant, positive clusters were detected for gamma-alpha coupling in midline-to-posterior channels [$t_{cluster}(66) = 16.612$, $p < 0.001$] and gamma-beta coupling across the majority of channels [$t_{cluster}(66) = 32.485$, $p < 0.001$].

Analyses of frequency modulation showed delta accelerated, while theta, alpha, and beta decelerated, with gamma occupying an intermediate position (Supplementary Fig. 6). The converging results suggest that harmonic locking is sensitive to cognitive demand and task-related arousal because they modulated instantaneous frequency of the various rhythms towards coupling (e.g. accelerating delta and decelerating theta).

The effect of breathing frequency, as an index of task-related arousal, echoed that of cognitive demand. System-wide harmonic locking increased, with hierarchical patterns emerging through the acceleration of lower-frequency rhythms and the deceleration of higher-frequency rhythms. This parallelism is intuitive as cognitive demand and physiological arousal are intrinsically linked (Grassmann et al., 2016). It leads one to hypothesize a mediation model whereby physiological arousal may account for part of cognitive demand's effect on harmonic locking. This is assessed in the Supplementary Materials (Supplementary Fig. 7).

III. Experiment 2

Prior work has shown that harmonic locking, frequency alignment between rhythms, is modulated by cognitive demand, physiological arousal, and indices of subjective distress. Experiment 1 broadened this scope, demonstrating that cognitive demand and task-related arousal enhanced harmonic locking within and between the brain and cardiorespiratory system. In both cases, coupling was organized hierarchically: cardiorespiratory rhythms aligned with low-frequency brain rhythms, which in turn aligned with higher-frequency brain activity. Experiment 2 extends this framework by testing the third predictor: subjective distress. Distress conceptually overlaps with demand and arousal, adds a state valence dimension unexamined in brain-body coupling, and can potentially unify the

constructs as constituent elements of task-related stress. Further, the assessment of negatively-valenced affective states can begin to delineate whether the coupling enhancements in high-demand states reflect adaptive challenge or maladaptive threat (Blascovich & Tomaka, 1996).

Theories of emotion, such as the James-Lange theory of emotion (James, 1894), and appraisal theories more broadly (Seth, 2013) argue that emotional experience emerges from the perception of bodily states or, in more recent formulations, from the inference of the causes of bodily states. Affect, the physiological instantiation of emotional processes, is classically described in two dimensions: arousal and valence (Russel, 1980). Physiological arousal, assessed in Experiment 1, enhanced brain-body coupling. State valence, the spectrum between misery and pleasure, is unstudied in this form of cross-frequency coordination, though there is some evidence suggesting a link to anxiogenic traits (Alaerts et al., 2021, 2024). Experiment 2 therefore examined the role of affective valence in modulating harmonic locking.

Methods

Experimental Design

Experiment 2 employed a within-subjects design with three conditions: rest, negative mood induction, and positive mood induction. In the resting-state condition, participants were instructed to remain relaxed

and engage in unguided thought during a 12-minute recording. The mood induction procedures followed Jefferies et al. (2008). For both the negative and positive conditions, participants were presented with an affective keyword ("sad" or "happy") and asked to recall and relive a personal memory associated with that emotion for 12 minutes. Each induction was accompanied by music validated for mood induction, presented through the participant-facing laptop speakers, also as described in Jefferies et al. (2008)[7]. Before and after each condition, participants completed the Positive and Negative Affect Schedule Short Form (PANAS-SF; Mackinnon et al., 1999) –the 10-item variant of the PANAS– to index their affective valence. The experiment was approved by the Institutional Review Board of the University of California, Santa Barbara.

Participants

40 healthy, neurotypical individuals were recruited from the student population for a single-session experiment conducted in the Memory Emotion Thought Awareness (META) Laboratory at the University of California, Santa Barbara. Eligibility criteria excluded individuals with a history of cardiorespiratory, gastrointestinal, or neuropsychiatric disorders, as well as traumatic brain injury. Data from three participants were excluded due to prevalent artifacts in their recordings, yielding a sample of

7 The negative mood induction included Mozart's *Eine Kleine Nachtmusik Allegro* (6:08), Bach's *Brandenburg Concerto #3 Allegro* (4:48), and Tchaikovsky's *The Nutcracker Waltz of the Flowers* (6:49). The positive mood induction included Chopin's *Prelude, Op. 28, No. 4* (2:34) and Albinoni's *Adagio in G Minor* (11:31). The music selection in the mood induction conditions was delivered in a random order.

37 participants (21 female; mean age = 20.05 years; mean BMI = 23.94 kg/m^2).

Data Collection

EEG was recorded using a 38-channel ElectroCap International Cap (10-10 system) and sampled at 256 Hz with two Neurofield Q21 amplifiers configured together for the 38-channel variation. Neurofield Suite recording software was used for data recordings and data files were exported in European Data Format (EDF) for pre-processing in later steps. The cardiorespiratory recording equipment and temporal synchronization procedures to align both amplifiers were consistent with Experiment 1.

Data Pre-Processing

Preprocessing procedures in Experiment 2 were identical to those in Experiment 1, with two exceptions: cardiorespiratory data were downsampled from 1000 Hz to 256 Hz to match the EEG sampling rate, and flat or dead channels were identified using EEGLAB's Clean_rawdata plug-in[8] (Kothe & Makeig, 2013).

Harmonic Locking Calculation

8 Clean_rawdata parameters were set as follows: 1) channels were removed if flat for more than 5 seconds, 2) maximum acceptable high-frequency noise standard deviation = 4, and 3) minimum acceptable correlation with nearby channels = 0.65.

Procedures were identical to those used in Experiment 1, with modifications made for the new 256 Hz sampling rate.

Statistical Analysis

A similar multi-stage analysis strategy was applied in this experiment. To test whether fluctuations in affective valence predicted coupling, post-condition positive and negative affect factor scores were regressed on system-wide harmonic locking while controlling for pre-condition responses[9]. Directional hypotheses were pre-registered (Young et al., 2024): negatively-valenced affect, under the auspices of a stress-based account, was expected to enhance harmonic locking, whereas positively-valenced affect was expected to suppress it. Models were then repeated for each rhythm pair[10]. A post hoc analysis tested change scores for individual PANAS-SF items (e.g., change in “Alert”) to further narrow which aspects of phenomenology drive coupling. These analyses were conducted using two-tailed tests. Condition-related differences in cross-frequency coupling are discussed in the Supplementary Materials (Supplementary Fig. 20). All of the above were assessed using cluster-based permutation models. The non-

---

9 The linear regression formula was structured like so:
Harmonic Incidence ~ Post-Condition Affect Scores (Positive or Negative) + Pre-Condition Affect Scores + Rhythm Pair Label (categorical covariate) + Condition (categorical covariate) + (Post-Condition Affect Scores | Participant ID)

10 The linear regression formula was structured like so:
Harmonic Incidence ~ Post-Condition Affect Scores (Positive or Negative) + Pre-Condition Affect Scores + Condition (categorical covariate) + (Post-Condition Affect Scores | Participant ID)

spatialized analyses such as the heart-breath harmonic locking were analyzed using parametric methods.

Secondary Analyses

Consistent with Experiment 1, we assessed the specificity of cross-frequency interactions as well as affective frequency modulation.

Results and Discussion

Cardiorespiratory Frequency Modulation & Heart-Breath Harmonic Locking

Changes in state negative [$\beta = 0.002$, $t(65.963) = 0.857$, $p = 0.395$] or positive affect factor scores [$\beta = -0.003$, $t(67.591) = -1.418$, $p = 0.161$] failed to modulate heart rate. Neither negative [$\beta = 0.001$, $t(86.768) = 0.326$, $p = .745$] nor positive affect [$\beta = -0.0001$, $t(89.869) = -0.087$, $p = 0.931$] predicted breathing frequency. Changes in negative [$\beta = 0.001$, $t(83.721) = 0.051$, $p = 0.960$] and positive affect [$\beta = -0.004$, $t(87.147) = -0.261$, $p = 0.795$] were not significant predictors of heart-breath coupling.

Harmonic Locking is Enhanced by Negatively-Valenced Affect

A significant, positive cluster was identified over posterior regions, indicating that increases in negatively-valenced affect were associated with greater system-wide harmonic locking, $t_{cluster}(2038) = 10.324$, $p < 0.001$

(Fig. 5). In contrast, the analysis of the change in positively-valenced affect revealed no significant clusters and no individual channel effects. The effect of negatively-valenced affect, although hypothesized and supported by the data, is quite limited relative to previous findings. One possible reason for this discrepancy is the variance in the associated arousal for each item. This discrepancy, in part, motivated the subsequent item-level post hoc tests.

The rhythm-pair models revealed a novel pattern. As negatively-valenced affect increased, coupling of theta with alpha [$t_{cluster}(99) = 48.499$, $p < 0.001$] and gamma [$t_{cluster}(99) = 90.540$, $p < 0.001$] was enhanced across the majority of channels. Theta appeared to supplant delta as the central binding rhythm, consistent with the well-established role of theta in coordinating higher-frequency EEG during memory tasks (Sauseng et al., 2009; Alekseichuk et al., 2016) and aligning with the memory-based design of Experiment 2.

The frequency modulation analysis indicated negatively-valenced affect-related accelerations in the gamma and alpha bands, accompanied by a deceleration in the theta band (Supplementary Fig. 14). Coupling of theta to alpha and gamma appeared to emerge through this coordinated modulation of both higher- and lower-frequency rhythms. These findings diverge, in part, from the demand- and arousal-related effects in Experiment 1, where coupling low-frequency rhythms accelerated to align with decelerating higher-frequency activity. Experiment 2 updates this framework, suggesting that enhanced coupling arises from reciprocal

modulation across frequencies rather than unidirectional adjustment of the binding rhythm alone.

In summary, state negative, but not positive, affect factor scores were associated with enhanced harmonic locking. Theta supplanted delta as the binding low-frequency rhythm, coupling with alpha and gamma, likely reflecting the memory-based tasks of Experiment 2. Frequency modulation analyses showed that this effect was driven by high-frequency acceleration and low-frequency deceleration, updating the interpretation from Experiment 1 to include reciprocal frequency adjustments in either direction.

Harmonic Locking is Enhanced by Threat-Related Phenomenology

To identify which aspects of the negative affect factor account for brain-body synchrony, models were conducted at the item level for each PANAS-SF item (e.g. the effect of increasing “Nervous” response). Of the 10 items, only two yielded significant clusters or any significant channels at all: “Afraid” and “Scared.” Increases in one’s “Afraid” [$t_{cluster}(2038) = 24.775$, $p < 0.001$] and “Scared” [$t_{cluster}(2038) = 36.613$, $p < 0.001$] responses, separately, enhanced harmonic locking in a cluster consisting of midline and posterior channels (Fig. 6). The items load on to the negative affect factor but are characterized as involving greater arousal relative to other negative affect items (e.g. “Nervous”). This suggests that system-wide harmonic locking is enhanced by phenomenology at the intersection of

negatively-valenced affect and heightened arousal, with the predictive items converging to describe responses to threat.

The Afraid-related models conducted for each rhythm pair depicted a hierarchical nesting of high- and low-frequency anchored by the theta band (Fig. 7). First, as Afraid responses increased, theta-heart coupling increased in the majority of channels [$t_{cluster}(99) = 98.455$, $p < 0.001$]. Second, theta coupled to all comparatively higher-frequency rhythms. Significant, positive clusters were identified for alpha-theta [$t_{cluster}(99) = 145.436$, $p < 0.001$] and beta-theta coupling [$t_{cluster}(99) = 92.092$, $p < 0.001$] in the majority of channels, and gamma-theta coupling in separate left- [$t_{cluster}(2038) = 26.880$, $p < 0.001$] and right-hemisphere clusters [$t_{cluster}(99) = 39.045$, $p < 0.001$]. Theta supplanted delta as the binding low-frequency rhythm. In fact, significant, negative clusters were identified for delta-heart coupling in separate left- [$t_{cluster}(99) = -24.919$, $p < 0.001$] and right-hemisphere clusters [$t_{cluster}(99) = -13.378$, $p < 0.001$], alpha-delta in the left-hemisphere [$t_{cluster}(99) = -24.993$, $p < 0.001$], and beta-delta coupling also in a left-hemisphere cluster [$t_{cluster}(99) = -23.741$, $p < 0.001$]. However, delta-breath coupling exhibited a significant, positive cluster consisting of the majority of channels [$t_{cluster}(99) = 61.371$, $p < 0.001$]. There were two novel findings. First, the alpha band coupled to the heart rate [$t_{cluster}(99) = 163.973$, $p < 0.001$] and decoupled from the gamma band in the majority of channels [$t_{cluster}(99) = -57.773$, $p < 0.001$]. Second, a significant, negative cluster was identified for gamma-beta coupling in the right-hemisphere [$t_{cluster}(99) =$

-16.671, p = 0.002]. The results, though not without noise, indicate a pattern of hierarchical organization whereby the heart coupled to theta and theta, in turn, coupled to comparatively higher-frequency activity. The former is notable given the heart's role in modulating affect via its rate variability (Chalmers et al., 2014).

The Scared-related models conducted for each rhythm pair illustrated a similar theta-based organization. As Scared responses increased, theta-heart coupling increased in the left-hemisphere [$t_{cluster}(99) = 14.022$, $p < 0.001$]. Significant, positive clusters were identified for alpha-theta coupling in the left hemisphere [$t_{cluster}(99) = 17.127$, $p < 0.001$] and gamma-theta coupling in the majority of channels [$t_{cluster}(99) = 39.227$, $p < 0.001$]. A decoupling of gamma and alpha was similarly found in left-frontal channels [$t_{cluster}(99) = -11.337$, $p < 0.001$].

The frequency modulation analysis depicted a gamma, beta, and alpha acceleration, paired with a corresponding theta deceleration (Supplementary Fig. 17; for brevity, only Afraid is plotted). Heart rate and breathing frequency were tested as functions of Afraid and Scared given the enhanced theta-heart coupling. Heart rate accelerated with increases in both "Afraid" [$\beta = 0.065$, $t(79.033) = 2.182$, $p = 0.032$] and "Scared" scores [$\beta = 0.032$, $t(66.532) = 2.547$, $p = 0.013$]. In contrast, neither breathing frequency nor heart-breath harmonic locking were modulated by either item. The stronger effect of Afraid relative to the negative affect factor is

explained by its greater modulation of frequency dynamics that favor cross-frequency coupling.

In summary, threat-related phenomenology (Afraid and Scared) –a negatively-valenced, high-arousal state– enhanced harmonic locking through a theta-based organization, with the heart coupling to theta and theta in turn synchronizing with higher-frequency activity. This was enabled by a coordinated acceleration and deceleration between lower- and higher-frequency activity. These results extend the findings of Experiment 1, showing that the hierarchical organization of brain-body coupling observed under cognitive demand and physiological arousal is similarly engaged when experiencing subjective distress. The three sets of findings converge on harmonic locking as a stress-responsive system in which cognitive resources are mobilized, physiology is activated, and subjective sense of threat is heightened.

IV. Experiment 3

Experiments 1 and 2 demonstrated that brain-body harmonic locking is driven by state stress. Cognitive demand, task-related arousal, and negatively-valenced affect each enhanced coupling, and together they can be unified as complementary components of the stress response to perceived threat, elicited by cognitive load or negatively-valenced memories. This aligns with prior findings in harmonic locking, such as the

association between alpha-theta coupling and indices of distress (Alaerts et al., 2021, 2024). It is also consistent with evidence that the cardiorespiratory rhythms modulate threat perception: fear-related stimuli presented during systole (Garfinkel et al., 2014) or inspiration (Zelano et al., 2016) are detected more rapidly than during other phases of the cardiac or respiratory cycle. If brain-body harmonic locking is a stress-responsive mechanism, then it should manifest in individual differences. If state stress, as elicited in the laboratory, enhanced cross-frequency coupling, then stress accumulated prior to the participant's laboratory session should likewise predict enhancements in system-wide coupling.

A second, tangential hypothesis assessed herein derived from the broader field of brain-body synchrony. As one substrate for brain-body integration, harmonic locking may index individual differences in interoception, the ability to perceive the internal state of the body (Craig, 2003). Heartbeat-evoked potentials (Pollatos & Schandry, 2004), gastric-alpha phase-amplitude coupling (Richter et al., 2017), and gastric-BOLD phase-locking (Rebollo et al., 2018) are mechanisms by which brain rhythms can entrain to bodily activity, thereby encoding visceral and somatic parameters (Young et al., 2022a). Although no studies have directly tied brain-body harmonic locking to interoception, the analysis is motivated by robust associations between interception and related modes of brain-body synchrony.

To assess individual differences in brain-body coupling, the data of Experiments 1 and 2 were pooled and participant self-reports of perceived stress and interoception were employed as predictors.

Methods

The pooled dataset consisted of 60 participants (34 females) with a mean age of 21.75 years and mean BMI of 24.09 kg/m^2. Meta-analysis was limited to the shared 19 channels (10-20 system). Prior to data collection participants completed two questionnaires, the Perceived Stress Questionnaire (PSQ) and the Three-domain Interoceptive Sensations Questionnaire (THISQ), whose responses were used as predictors in linear regression and submitted to cluster-based permutation models[11].

The Perceived Stress Questionnaire (PSQ) is a 30-item scale targeting stressful life circumstances in the preceding month (Levenstein et al., 1993). The scale consists of seven factors: fatigue (e.g. You feel tired), harassment (e.g. You find yourself in situation of conflict), irritability (e.g. You feel criticized or judged), lack of joy (e.g. You feel you're in a hurry), overload (e.g. You have too many things to do), tension (e.g. You feel mentally exhausted), and worries (e.g. You are afraid for the future). The Three-domain Interoceptive Sensations Questionnaire (THISQ) is an 18-item

---

11 The linear regression formula was structured like so for the system-wide models:
Harmonic Incidence ~ Predictor (PSQ or THISQ) + Rhythm Pair Label (categorical covariate) + Condition (categorical covariate) + Study (categorical covariate) + (1 | Participant ID)
And like so for individual rhythm-pair models:
Harmonic Incidence ~ Predictor (PSQ or THISQ) + Condition (categorical covariate) + Study (categorical covariate) + (1 | Participant ID)

scale targeting interoceptive sensibility (Vlemincx et al., 2021), one's personal account for how they experience their bodily sensations (Garfinkel et al., 2015). It comprises three factors: cardiorespiratory activation (e.g. During a light physical effort, I feel my heart beat), cardiorespiratory deactivation (e.g. When I come to rest, I feel my heart rate slow down), and gastroesophageal sensation (e.g. I feel when my bowels contract).

The design philosophy of the analysis is identical to that employed in the preceding experiments. Though the analysis was approached with a priori hypotheses, the system-wide models were conducted as non-directional having not been pre-registered.

Results and Discussion

Harmonic Locking is Enhanced by Individual Differences in Perceived Stress

Two significant, positive clusters were identified over frontal [$t_{cluster}(3410) = 7.423$, $p = 0.002$] and posterior cortices [$t_{cluster}(3410) = 17.453$, $p < 0.001$]. Participants who reported greater stressful life circumstances exhibited stronger system-wide harmonic locking than their less stressed counterparts, matching the topography of cognitive demand (Fig. 8; also see Fig. 1). Among the seven PSQ factors, only irritability, harassment, and tension failed to yield significant clusters, with overload most strongly accounting for system-wide coupling.

Results within each rhythm pair were highly consistent with negatively-valenced affect, indicating the pattern of coupling activated by state stress is likewise activated by latent stress. Theta showed stronger coupling with higher-frequency brain rhythms. Significant, positive clusters were identified for beta-theta coupling bilaterally [Left: $t_{cluster}(162) = 14.996$, $p < 0.001$; Right: $t_{cluster}(162) = 11.660$, $p < 0.001$] and gamma-theta coupling in the right hemisphere [$t_{cluster}(162) = 10.378$, $p = 0.001$]. Heart-breath coupling was not affected by perceived stress [$\beta = -0.034$, $t(101.759) = -0.086$, $p = 0.932$]. The theta-based pattern of low- to high-frequency coupling was enhanced as a function of latent stress, but the absence of cardiorespiratory involvement raises questions about whether stress primarily engages intra-brain rather than brain-body coordination. This, together with the apparent lack of brain-breath coupling in response to negatively-valenced affect, suggests that the bodily component of brain-body coupling may emerge more directly from the stress-related increase of physiological arousal.

The frequency modulation resembled that observed for negatively-valenced affect. Higher-frequency EEG accelerated as a function of latent stress, while the coupling theta band decelerated (Supplementary Fig. 23). Neither heart rate [$\beta = -0.012$, $t(165.559) = -0.114$, $p = 0.910$] nor breathing frequency [$\beta = -0.043$, $t(108.118) = -1.364$, $p = 0.175$] were affected by perceived stress, which likely accounts for the absence of brain-body coupling.

In summary, individual differences in perceived stress predicted stronger harmonic locking, echoing the theta-based organization observed under negatively-valenced affect but notably without cardiorespiratory involvement. The stress-related enhancement of harmonic locking was facilitated by a coordinated high-frequency acceleration and theta deceleration. The absence of perceived stress effects on heart rate or breathing frequency suggests that latent stress predominantly engages intra-brain coordination, and brain-body coupling likely arises from the related activation of physiological arousal as in the state-based manipulations of stress.

Harmonic Locking is Enhanced by Interoceptive Sensitivity to Increases in Physiological Arousal

A secondary hypothesis addressed interoception, since related brain-body synchrony indices track individual differences. Among the Three-Domain Interoceptive Sensations Questionnaire (THISQ) composite and factor scores assessed separately, only the cardiorespiratory activation factor explained variance in system-wide harmonic locking. Greater sensitivity to increases in physiological arousal predicted stronger harmonic locking in two bilateral clusters spanning the posterior cortex [Left: $t_{cluster}(3410) = 11.538$, $p < 0.001$; Right: $t_{cluster}(3410) = 7.695$, $p = 0.001$]. The cluster topography was similar to the posterior arousal-related clusters

observed in Experiment 1 (Fig. 9; see also Fig. 3), suggesting that dispositional sensitivity to increases in arousal may amplify the effects of state-based arousal manipulations on harmonic locking.

The analysis of each rhythm pair indicated a coupling pattern consistent with earlier experiments, but they also cemented a novel contrast. Greater sensitivity to increases in arousal was associated with enhanced harmonic locking between heart rate and theta [$t_{cluster}(162) = 70.947$, $p < 0.001$], alpha [$t_{cluster}(162) = 59.859$, $p < 0.001$], and beta in the majority of channels [$t_{cluster}(162) = 54.229$, $p < 0.001$]. Delta reprised its role as a binding rhythm, coupling with alpha in posterior channels [$t_{cluster}(162) = 12.261$, $p < 0.001$] and gamma in frontal channels [$t_{cluster}(162) = 10.762$, $p < 0.001$]. In addition, theta showed stronger coupling with gamma in bilateral clusters [Left: $t_{cluster}(162) = 16.399$, $p < 0.001$; Right: $t_{cluster}(162) = 15.522$, $p < 0.001$]. Heart-breath coupling was unaffected by cardiorespiratory activation scores [$\beta = -0.011$, $t(130.548) = -0.804$, $p = 0.423$]. Less interpretable effects included alpha decoupling from beta in frontal and central regions [$t_{cluster}(162) = -28.039$, $p < 0.001$] and enhanced alpha-gamma coupling across most channels [$t_{cluster}(162) = 47.258$, $p < 0.001$]. The delta-based organization involving strong cardiorespiratory-brain coupling enhanced by cognitive demand and task-related arousal was latently enhanced by dispositional sensitivity to increases in arousal. By contrast, analyses of state negatively-valenced affect and dispositional perceived stress revealed a theta-based, largely intra-brain coupling pattern. This

discrepancy is likely attributable to the limited ability of negatively-valenced affect and perceived stress to modulate delta or cardiorespiratory frequencies, relative to the manipulations of Experiment 1. It introduces the possibility of two modes of brain and body integration that index distinct elements of the stress response: the cognitive element of demand which promoted theta-based, intra-brain coupling and the cardiorespiratory response to stress which promoted delta-based, brain-body coupling.

Cardiorespiratory activation scores predicted an acceleration of gamma and beta frequencies and a deceleration of alpha and theta (Supplementary Fig. 26). Delta, in contrast, appeared to stabilize toward the middle of its spectrum. This departed slightly from the previous experiments, where enhanced coupling was driven by coordinated, oppositional modulation of lower- and higher-frequency activity. Here, enhanced delta coupling with theta, alpha, and gamma seems to have been enabled by delta's middle-ground positioning, allowing it to align with both accelerated and decelerated rhythms. In addition, cardiorespiratory activation scores were associated with an accelerated heart rate [$\beta = 0.016$, $t(165.235) = 4.471$, $p < 0.001$] but had no effect on breathing frequency [$\beta = -0.002$, $t(139.297) = -1.771$, $p = 0.078$]. cardiorespiratory-brain coupling appeared driven by cardiorespiratory acceleration even when EEG frequencies fluctuated in opposite directions.

In summary, individual differences in sensitivity to cardiorespiratory activation predicted enhanced harmonic locking, expressed through a delta-

based organization involving cardiorespiratory-brain coupling. Unlike state negatively-valenced affect or dispositional perceived stress, which primarily engaged theta-based intra-brain coupling, this finding highlights an important contrast in modes of integration: theta-anchored, intra-brain coupling appears linked to cognitive demand, whereas delta-anchored, brain-body coupling reflects the activation of physiological arousal. Distinct elements of the stress response engage distinct modes of brain and body coordination.

V. General Discussion

A recent theory proposed harmonic locking as a scale-invariant substrate whereby fast and slow rhythms of the brain and body may coordinate task-relevant activity as a unified system (Klimesch, 2018). Previous scholars have found that brain and cardiorespiratory rhythms increasingly promote this form of cross-frequency coupling as functions of cognitive demand and physiological arousal, though this research was limited to the alpha band. The present study extended the scope and affirmed the broader theoretical account by demonstrating that harmonic locking is not confined to disparate pairs of rhythms but instead emerged as a system-wide, hierarchically-organized property of brain-body coordination engaged by state and latent stress, encompassing the low-frequency, network-level to higher-frequency, cortically-generated brain rhythms.

Cognitive demand, task-related arousal, and negatively-valenced affect enhanced harmonic locking within and between the brain and cardiorespiratory system. The direction and topography of the effects were consistent between predictors suggesting a conceptual and functional overlap. Indeed, we proposed the three constructs may be unified as elements of the stress response whereby cognitive resources are mobilized, physiology is activated, and subjective distress is increased. A third, meta-analytical experiment found individual differences in perceived stress and interoceptive sensitivity to increases in arousal likewise enhanced harmonic locking, further corroborating its function as a state and latent stress-responsive mechanism.

Notably, harmonic locking appeared to be a hierarchical phenomenon: cardiorespiratory rhythms coupled to low-frequency, network-level brain rhythms and these rhythms, in turn, coupled to comparatively higher-frequency brain activity. This was enabled by a coordinated and opposite acceleration/deceleration of lower- and higher-frequency rhythms. By contrast, brain-cardiorespiratory coupling appeared to depend specifically on the acceleration of cardiorespiratory rhythms.

Lastly, the findings suggest that distinct elements of the stress response recruit distinct modes of brain and body synchrony, contingent on whether increases in arousal are elicited. The cognitive component of the stress response promoted intra-brain coupling anchored by the theta band,

whereas the bodily component of the stress response promoted brain-body coupling anchored by the delta band.

An emerging perspective within human neuroscience holds that cognitive dynamics are inseparable from the bodily systems that sustain and stimulate the brain (Thompson & Varela, 2001; Fuchs, 2009; Foglia & Wilson, 2013; Kluger et al., 2024). Rhythms of the heart, breath, and stomach have been shown to modulate neural networks, influence cognition, and shape phenomenology (Azzalini et al., 2019; Young et al., 2022a; Engelen et al., 2023). In parallel, contemporary theories of consciousness increasingly emphasize synchrony within and across nested spatiotemporal scales as a means for overcoming the combination problem (Hunt & Schooler, 2019; Riddle & Schooler, 2024). Brain-body synchrony thus sits at an intersection of related fields, offering a shared empirical language for investigating underlying systems responsible for homeostatic maintenance, allostatic forecasting, and embodied phenomenology. The present study offers a new layer to the shared account: the unity of brain and body –and, by extension, the embodied consciousness– is dynamic, waxing and waning with external constraints and individual dispositions.

Future Directions

While this study demonstrated strong associations between dimensions of stress and harmonic locking, and its results presented coherently across experiments, establishing causal direction from these

findings alone remains challenging. A greater sense of causality may be derived by manipulating levels of each predictor by, for example, presenting high vs. low demand (1-back vs. 3-back) or arousal conditions (rest vs. moderate exercise). The present research would benefit greatly from the latter as the constraining of breath within Experiment 1 plausibly may have confounded interpretations of “natural” arousal effects.

Our account of intra-brain and brain-body harmonic locking is stress-centric. State and latent stress elicited by perceived threat was associated with increased coupling between brain and cardiorespiratory rhythms, but to what end? Does it increase working memory capacity or the acuity of threat perception? The former is supported by evidence that alpha-theta harmonic locking improves working memory (Rodriguez-Larios et al., 2019). The latter possibility is consistent with evidence that fear-related stimuli are detected more rapidly when they coincide with specific phases of cardiorespiratory rhythms (Garfinkel et al., 2014; Zelano et al., 2016). The improved threat detection may be facilitated by the stress-related coupling of EEG to cardiorespiratory rhythms, particularly in posterior cortical regions housing visual centers, which consistently showed enhanced intra-brain and brain-body coupling across experiments.

Beyond speculating function, it is necessary to elucidate the direction of coupling. Analyses assessing the frequency modulation underlying the fluctuations in intra-brain harmonic locking indicated an oppositional modulation of the anchoring low-frequency rhythm (e.g. delta or theta) and

the comparatively higher-frequency rhythms it coupled to. Coupling of brain rhythms to cardiorespiratory rhythms seemed unilaterally decided by cardiorespiratory acceleration. Is the frequency modulation that facilitated coupling non-directional between rhythms or is it facilitated by the lower-frequency rhythm? For example, phase-amplitude coupling, a synchrony index applied to intra-brain and brain-body contexts, is explicitly directional whereby the phase of a lower-frequency rhythm modulates the excitability of a higher-frequency rhythm, but not vice versa (Tort et al., 2008).

A last, speculative question emerges in the wake of exciting work showing that the distinct brains of interacting individuals will synchronize together as a function of their interaction (Valencia & Froese, 2020; Young et al., 2022b). For example, inter-brain phase synchrony in dyads was greater when performing joint visual search tasks relative to individual tasks and inter-dyad differences in inter-brain synchrony predicted team performance (Szymanski et al., 2017). Instantaneous frequency is the first temporal derivative of the phase angles that are employed in phase-locking indices, raising the question if inter-brain phase synchrony is associated with the intra-brain and brain-body harmonic locking that is enabled by coordinated modulation of instantaneous frequency. Put differently, does the hierarchical nesting of cardiorespiratory, low-frequency, and high-frequency rhythms elicited by task demands facilitate that organism's ability to couple with a cooperating conspecific? It would be consistent with the growing link between empathy and interoception (Fukushima et al., 2010;

Mul et al., 2018), the latter relying on brain-body coupling in various forms, yet the correlation between alpha-theta harmonic locking and social impairment in autistic cohorts would suggest otherwise (Alaerts et al., 2024). There is clear potential in bridging brain-body and inter-brain synchrony.

VI. Tables and Figures

Figure 1.

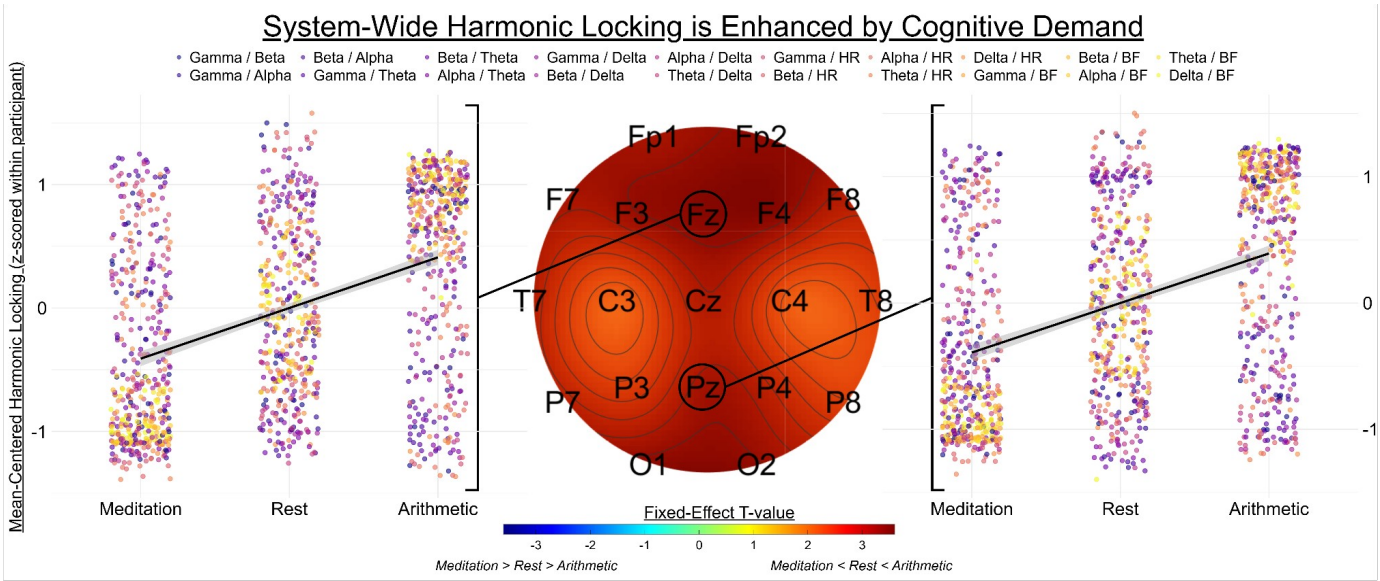

Note. This figure presents 1) in the center, the topographical distribution of cognitive demand's fixed-effect t-values and labels of channels within the significant cluster; and 2) in the margins, the harmonic incidence rates, controlled for condition length differences, from channels central to their respective foci. The latter has been normalized within participants to unify the y-axis across the different rhythm pairs, mean-centered to reflect the

within-subjects nature of the data, and color-coded continuously according to the frequency of the denominator and numerator of the pairing (e.g. coupling between high-frequency EEG is plotted in darker purple and coupling of EEG to cardiorespiratory rhythms is plotted in yellow). System-wide harmonic locking increases as a function of cognitive demand (meditation < rest < arithmetic). It appears, in the margin plots, to be driven particularly by cardiorespiratory-brain and low- to high-frequency coupling.

Figure 2.

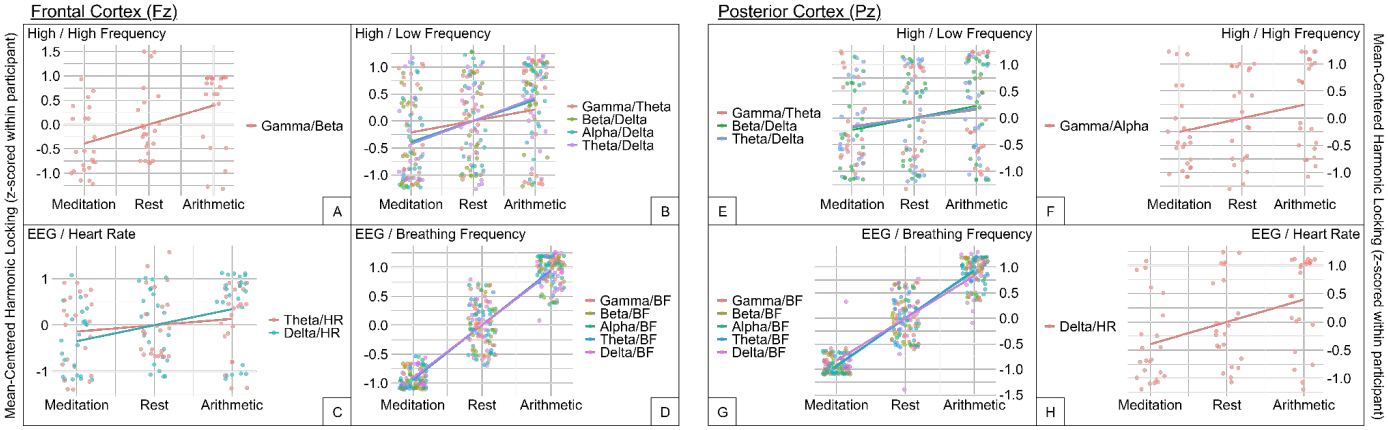

Note. Each panel depicts the harmonic incidence of rhythm pairings whose significant clusters included the listed channel –controlling for condition length differences, normalized within participants, and mean-centered. A hierarchical pattern of interaction appears to emerge whereby, as a function of cognitive demand, cardiorespiratory rhythms couple to low-frequency, network-level rhythms (i.e. delta) and higher-frequency EEG couples to delta.

Figure 3.

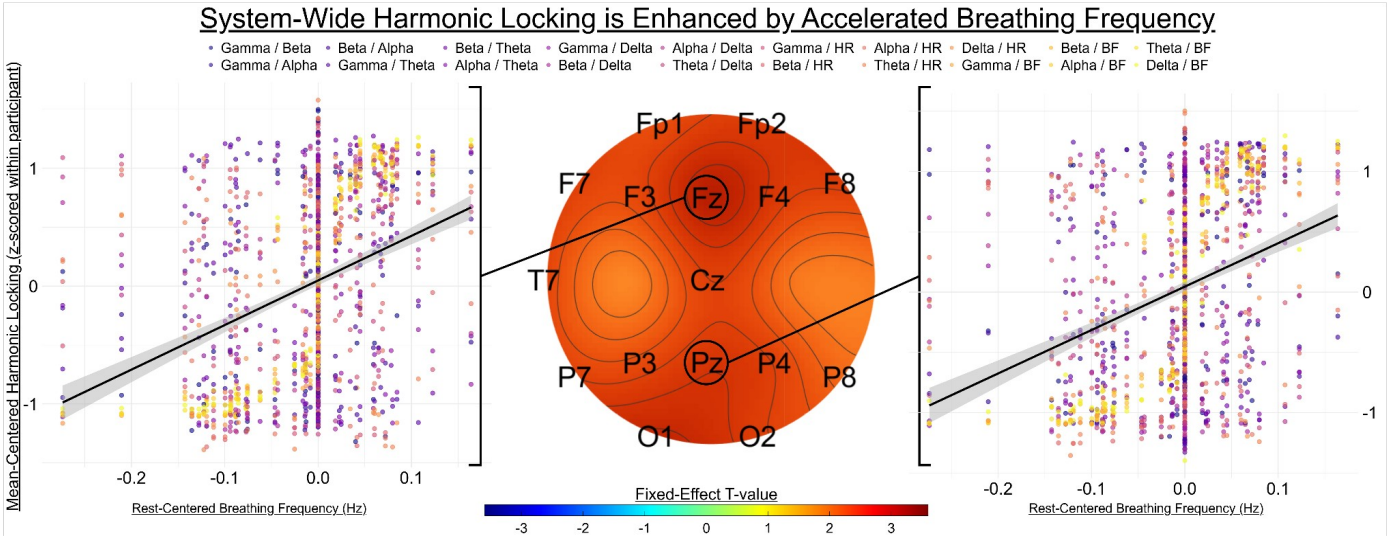

Note. This figure presents 1) in the center, the topographical distribution of breathing frequency's fixed-effect t-values and labels of channels within the significant cluster; and 2) in the margins, the harmonic incidence rates, controlled for condition length differences, from channels central to their respective foci. As breathing frequency accelerates, system-wide harmonic locking is enhanced in frontal and posterior cortices. The effect, though, is more limited, both in spatial distribution and effect, relative to that of cognitive demand.

Figure 4.

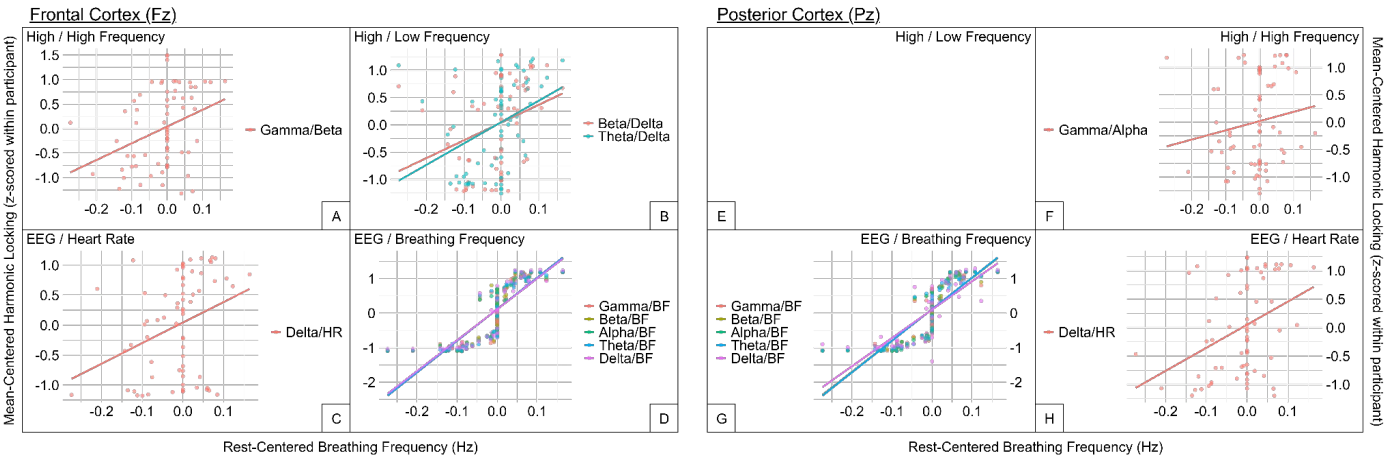

Note. Each panel depicts the harmonic incidence of rhythm pairings whose significant clusters included the listed channel –controlling for condition length differences, normalized within participants, and mean-centered. Fluctuations in mean breathing frequency most strongly account for coupling between itself and EEG. Nested upon that, similar to the effect of cognitive demand, is the enhancement of coupling between low- and high-frequency EEG, though this is limited to the frontal cortex.

Figure 5.

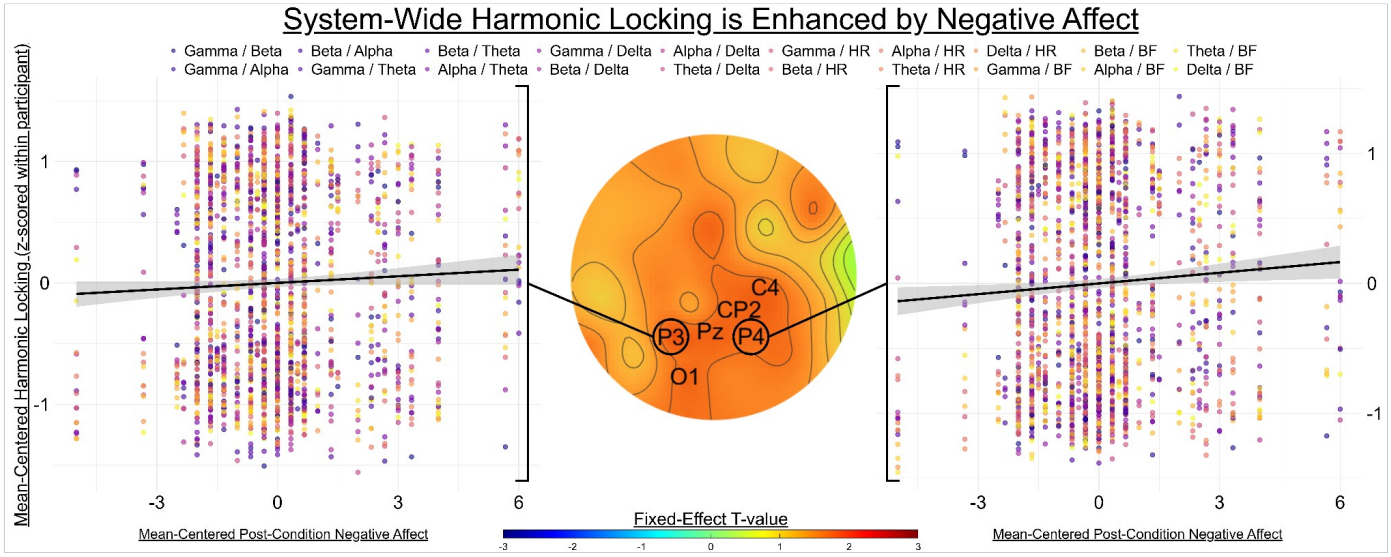

Note. The topographical plot in the center depicts the distribution of fixed-effect t-values of post-condition negative affect factor scores across the scalp after controlling for pre-condition responses. The margin plots depict the electrode-level data likewise controlling for pre-condition responses. As one's negatively-valenced –but not positively-valenced– affect increased, system-wide harmonic locking increased in a cluster that is consistent in topography with the posterior foci identified in Experiment 1. The effect, though, is far less extensive than cognitive demand or task-related arousal, and this may be partially explained by the heterogeneity in the arousal associated with negative affect factor items (e.g. "Scared" is characterized by greater arousal than "Nervous").

Figure 6.

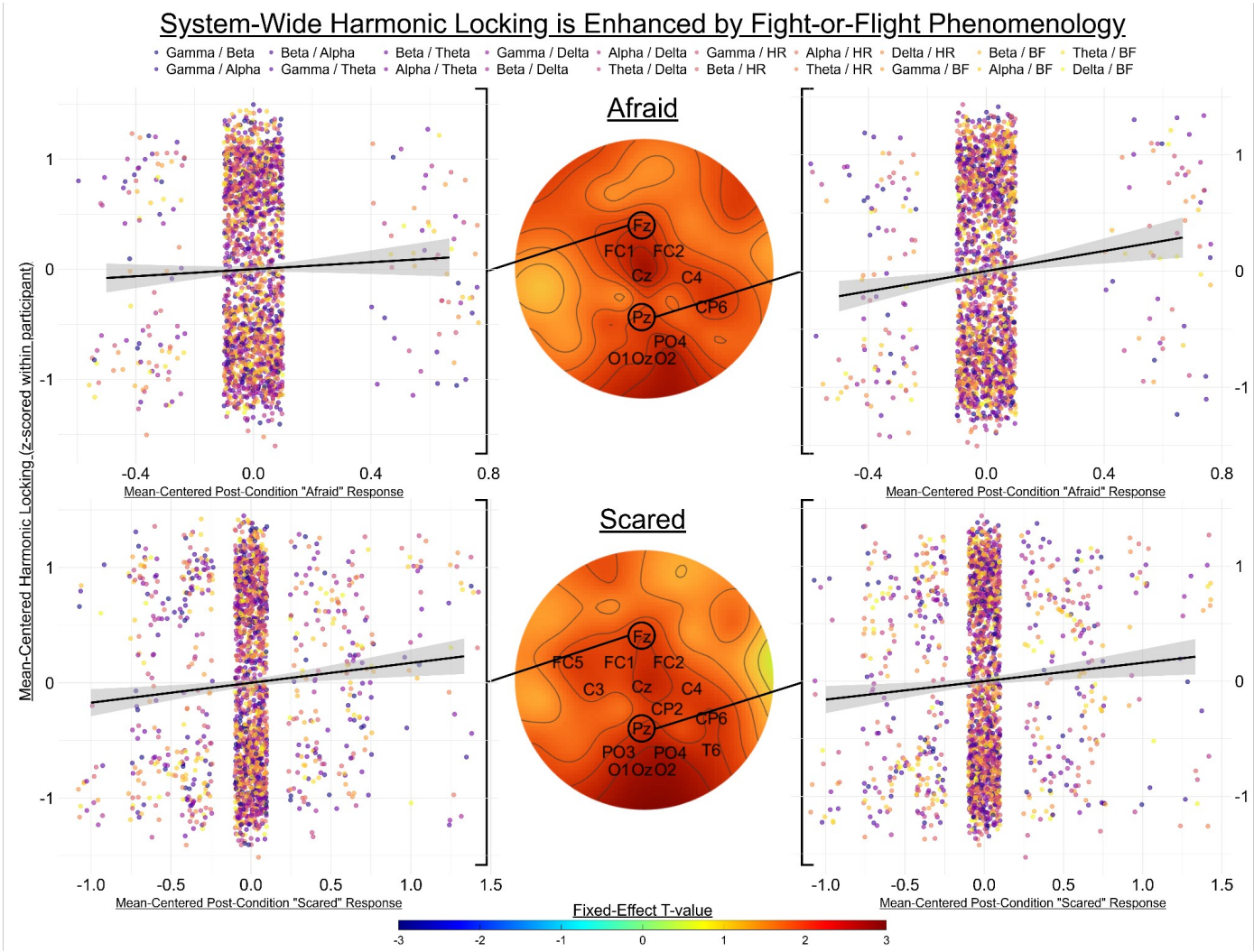

Note. The only two negative affect items, or any PANAS-SF items for that matter, that accounted for system-wide harmonic locking were items "Afraid" and "Scared." As one's responses to either of these items increased, system-wide coupling was enhanced in a cluster strongly resembling the frontal and posterior foci identified in Experiment 1. The converging direction and distribution of cognitive demand, task-related arousal, and threat-related phenomenology on system-wide harmonic locking suggests a conceptual and functional overlap. To unify the constructs, it is likely the system-wide enhancements to harmonic locking

are driven by state stress of which cognitive demand, physiological arousal, and subjective distress are aspects of.

Figure 7.

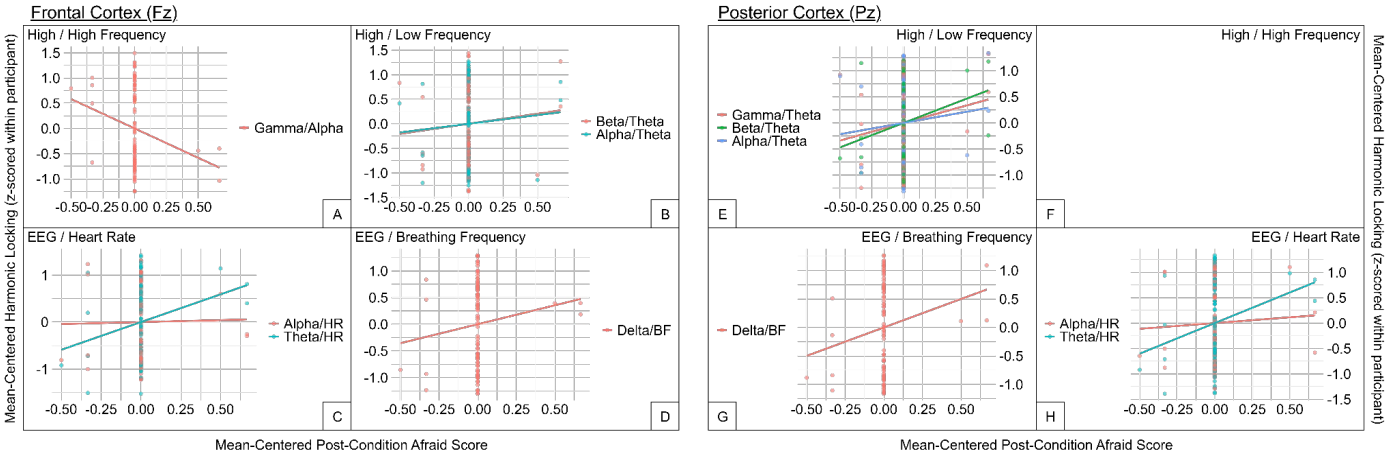

Note. Each panel depicts the harmonic incidence of rhythm pairings whose significant clusters included the listed channel –controlling for pre-condition responses, normalized within participants, and mean-centered. Contrasting the results of Experiment 1, the hierarchical organization of cardiorespiratory and EEG rhythms is supported by the theta band, supplanting the delta band. This is partially explained by the memory-task design of Experiment 2.

Figure 8.

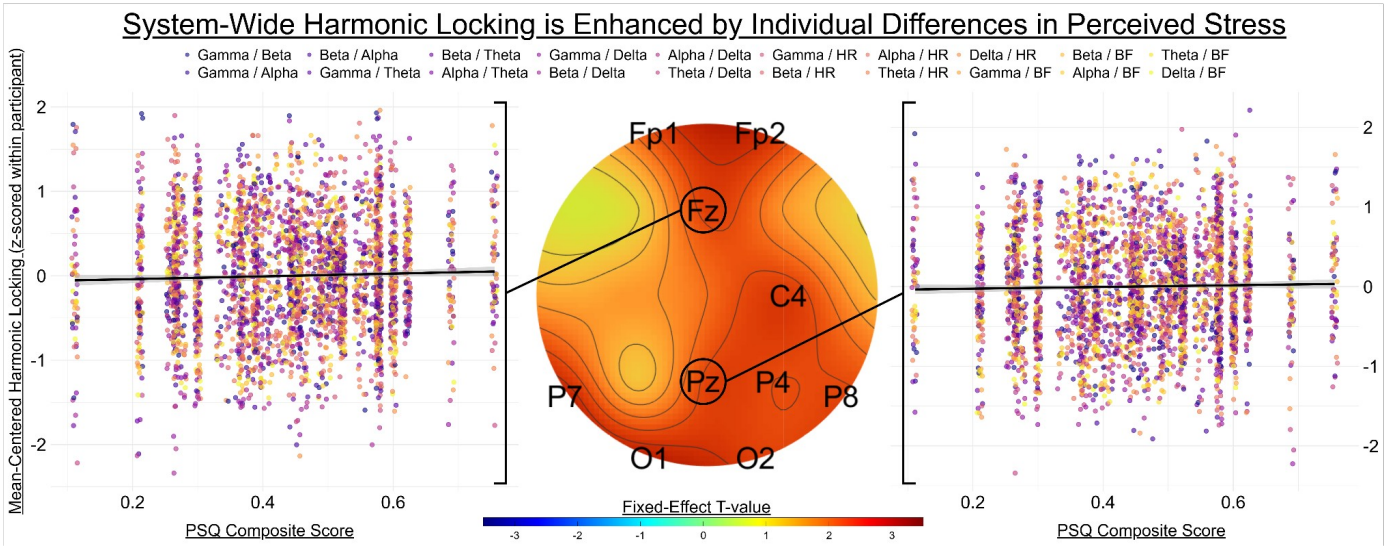

Note. Participants reporting greater stress, as indexed by the Perceived Stress Questionnaire (PSQ), in the 30 days prior to testing exhibited stronger system-wide harmonic locking than their less-stressed counterparts. The topographical distribution closely recapitulates the effects of cognitive demand (Fig. 2), suggesting convergence between state and dispositional stress. Among PSQ factors, overload most strongly predicted coupling, corroborating the interpretation of harmonic locking as a stress-responsive mechanism.

Figure 9.

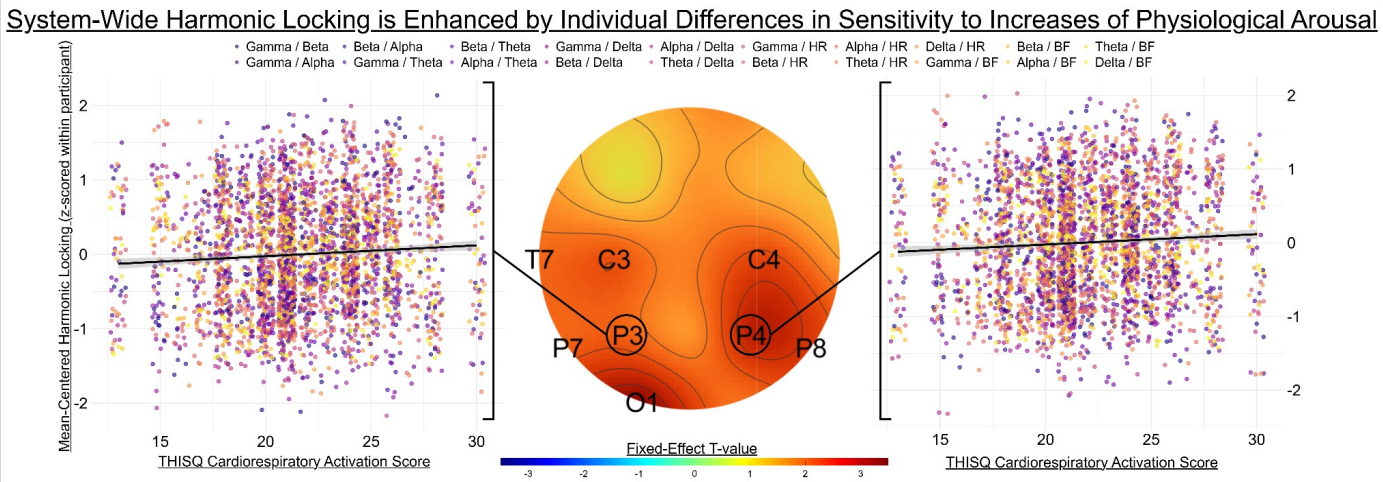

Note. Topographical plots show two significant bilateral posterior clusters where greater interoceptive sensitivity to increases in arousal predicted stronger harmonic locking. The distribution closely resembles the posterior arousal-related clusters identified in Experiment 1. These individual differences align with the stress-centric hypothesis advanced here, consistent with the premise that enhancements to harmonic locking under increased physiological arousal reflect the cardiorespiratory activation elicited by the stress response.

VII. References

1. Alaerts, K., Moerkerke, M., Daniels, N., Zhang, Q., Grazia, R., Steyaert, J., ... & Boets, B. (2024). Chronic oxytocin improves neural decoupling at rest in children with autism: an exploratory RCT. *Journal of Child Psychology and Psychiatry*, *65*(10), 1311-1326.

2. Alaerts, K., Taillieu, A., Prinsen, J., & Daniels, N. (2021). Tracking transient changes in the intrinsic neural frequency architecture: Oxytocin facilitates non-harmonic relationships between alpha and theta rhythms in the resting brain. *Psychoneuroendocrinology*, *133*, 105397.

3. Alekseichuk, I., Turi, Z., De Lara, G. A., Antal, A., & Paulus, W. (2016). Spatial working memory in humans depends on theta and high gamma synchronization in the prefrontal cortex. *Current biology*, *26*(12), 1513-1521.

4. Azzalini, D., Rebollo, I., & Tallon-Baudry, C. (2019). Visceral signals shape brain dynamics and cognition. *Trends in cognitive sciences*, *23*(6), 488-509.

5. Blascovich, J., & Tomaka, J. (1996). The biopsychosocial model of arousal regulation. In *Advances in experimental social psychology* (Vol. 28, pp. 1-51). Academic Press.

6. Canolty, R. T., & Knight, R. T. (2010). The functional role of cross-frequency coupling. *Trends in cognitive sciences*, *14*(11), 506-515.

7. Chalmers, J. A., Quintana, D. S., Abbott, M. J. A., & Kemp, A. H. (2014). Anxiety disorders are associated with reduced heart rate variability: a meta-analysis. *Frontiers in psychiatry*, *5*, 80.

8. Cohen, M. X. (2014). Fluctuations in oscillation frequency control spike timing and coordinate neural networks. *Journal of Neuroscience*, *34*(27), 8988-8998.

9. Craig, A. D. (2003). Interoception: the sense of the physiological condition of the body. *Current opinion in neurobiology*, *13*(4), 500-505.

10. Dehaene, S. (2014). *Consciousness and the brain: Deciphering how the brain codes our thoughts*. Penguin.

11. Delorme, A., & Makeig, S. (2004). EEGLAB: an open source toolbox for analysis of single-trial EEG dynamics including independent component analysis. *Journal of neuroscience methods*, *134*(1), 9-21.

12. Engelen, T., Solcà, M., & Tallon-Baudry, C. (2023). Interoceptive rhythms in the brain. *Nature Neuroscience*, *26*(10), 1670-1684.

13. Fields, R. D. (2020). *Electric Brain: How the New Science of Brainwaves Reads Minds, Tells Us How We Learn, and Helps Us Change for the Better*. BenBella Books.

14. Foglia, L., & Wilson, R. A. (2013). Embodied cognition. *Wiley Interdisciplinary Reviews: Cognitive Science*, *4*(3), 319-325.

15. Fuchs, T. (2009). Embodied cognitive neuroscience and its consequences for psychiatry. *Poiesis & Praxis*, *6*(3), 219-233.

16. Fukushima, H., Terasawa, Y., & Umeda, S. (2011). Association between interoception and empathy: evidence from heartbeat-evoked brain potential. *International Journal of Psychophysiology*, *79*(2), 259-265.

17. Garfinkel, S. N., Minati, L., Gray, M. A., Seth, A. K., Dolan, R. J., & Critchley, H. D. (2014). Fear from the heart: sensitivity to fear stimuli depends on individual heartbeats. *Journal of Neuroscience*, *34*(19), 6573-6582.

18. Garfinkel, S. N., Seth, A. K., Barrett, A. B., Suzuki, K., & Critchley, H. D. (2015). Knowing your own heart: distinguishing interoceptive accuracy from interoceptive awareness. *Biological psychology*, *104*, 65-74.

19. Grassmann, M., Vlemincx, E., Von Leupoldt, A., Mittelstädt, J. M., & Van den Bergh, O. (2016). Respiratory changes in response to cognitive load: A systematic review. *Neural plasticity*, *2016*(1), 8146809.

20. Gross, M., Raynes, S., Schooler, J. W., Guo, E., & Dobkins, K. (2024). When is a wandering mind unhappy? The role of thought valence. *Emotion*.

21. Helfrich, R. F., Huang, M., Wilson, G., & Knight, R. T. (2017). Prefrontal cortex modulates posterior alpha oscillations during top-down guided visual perception. *Proceedings of the National Academy of Sciences*, *114*(35), 9457-9462.

22. Hunt, T., & Schooler, J. W. (2019). The easy part of the hard problem: a resonance theory of consciousness. *Frontiers in Human Neuroscience*, *13*, 447026.

23. Hyafil, A., Giraud, A. L., Fontolan, L., & Gutkin, B. (2015). Neural cross-frequency coupling: connecting architectures, mechanisms, and functions. *Trends in neurosciences*, *38*(11), 725-740.

24. James, W. (1894). Discussion: The physical basis of emotion. *Psychological review*, *1*(5), 516.

25. Jefferies, L. N., Smilek, D., Eich, E., & Enns, J. T. (2008). Emotional valence and arousal interact in attentional control. *Psychological science*, *19*(3), 290-295.

26. Klimesch, W. (2013). An algorithm for the EEG frequency architecture of consciousness and brain body coupling. *Frontiers in human neuroscience*, *7*, 766.

27. Klimesch, W. (2018). The frequency architecture of brain and brain body oscillations: an analysis. *European Journal of Neuroscience*, *48*(7), 2431-2453.

28. Kluger, D. S., Allen, M. G., & Gross, J. (2024). Brain–body states embody complex temporal dynamics. *Trends in Cognitive Sciences*, *28*(8), 695-698.

29. Kothe, C. A., & Makeig, S. (2013). BCILAB: a platform for brain–computer interface development. *Journal of neural engineering*, *10*(5), 056014.

30. Lachaux, J. P., Rodriguez, E., Martinerie, J., & Varela, F. J. (1999). Measuring phase synchrony in brain signals. *Human brain mapping*, *8*(4), 194-208.

31. Lakatos, P., Shah, A. S., Knuth, K. H., Ulbert, I., Karmos, G., & Schroeder, C. E. (2005). An oscillatory hierarchy controlling neuronal excitability and stimulus processing in the auditory cortex. *Journal of neurophysiology*, *94*(3), 1904-1911.

32. Levenstein, S., Prantera, C., Varvo, V., Scribano, M. L., Berto, E., Luzi, C., & Andreoli, A. (1993). Development of the Perceived Stress Questionnaire: a new tool for psychosomatic research. *Journal of psychosomatic research*, *37*(1), 19-32.

33. Mackinnon, A., Jorm, A. F., Christensen, H., Korten, A. E., Jacomb, P. A., & Rodgers, B. (1999). A short form of the Positive and Negative Affect Schedule: Evaluation of factorial validity and invariance across demographic variables in a community sample. *Personality and Individual differences*, *27*(3), 405-416.

34. Maris, E., & Oostenveld, R. (2007). Nonparametric statistical testing of EEG-and MEG-data. *Journal of neuroscience methods*, *164*(1), 177-190.

35. Mul, C. L., Stagg, S. D., Herbelin, B., & Aspell, J. E. (2018). The feeling of me feeling for you: Interoception, alexithymia and empathy in autism. *Journal of autism and developmental disorders*, *48*(9), 2953-2967.

36. Oostenveld, R., Fries, P., Maris, E., & Schoffelen, J. M. (2011). FieldTrip: open source software for advanced analysis of MEG, EEG,

and invasive electrophysiological data. *Computational intelligence and neuroscience*, *2011*(1), 156869.

37. Palva, J. M., & Palva, S. (2018). Functional integration across oscillation frequencies by cross-frequency phase synchronization. *European Journal of Neuroscience*, *48*(7), 2399-2406.

38. Pion-Tonachini, L., Kreutz-Delgado, K., & Makeig, S. (2019). ICLabel: An automated electroencephalographic independent component classifier, dataset, and website. *NeuroImage*, *198*, 181-197.

39. Pollatos, O., & Schandry, R. (2004). Accuracy of heartbeat perception is reflected in the amplitude of the heartbeat-evoked brain potential. *Psychophysiology*, *41*(3), 476-482.

40. Rassi, E., Dorffner, G., Gruber, W., Schabus, M., & Klimesch, W. (2019). Coupling and decoupling between brain and body oscillations. *Neuroscience Letters*, *711*, 134401.

41. Rebollo, I., Devauchelle, A. D., Béranger, B., & Tallon-Baudry, C. (2018). Stomach-brain synchrony reveals a novel, delayed-connectivity resting-state network in humans. *elife*, *7*, e33321.

42. Richter, C. G., Babo-Rebelo, M., Schwartz, D., & Tallon-Baudry, C. (2017). Phase-amplitude coupling at the organism level: The amplitude of spontaneous alpha rhythm fluctuations varies with the phase of the infra-slow gastric basal rhythm. *NeuroImage*, *146*, 951-958.

43. Riddle, J., & Schooler, J. W. (2024). Hierarchical consciousness: The nested observer windows model. *Neuroscience of Consciousness*, *2024*(1), niae010.

44. Riddle, J., McFerren, A., & Frohlich, F. (2021). Causal role of cross-frequency coupling in distinct components of cognitive control. *Progress in Neurobiology*, *202*, 102033.

45. Rodriguez-Larios, J., & Alaerts, K. (2019). Tracking transient changes in the neural frequency architecture: harmonic relationships between theta and alpha peaks facilitate cognitive performance. *Journal of Neuroscience*, *39*(32), 6291-6298.

46. Rodriguez-Larios, J., Faber, P., Achermann, P., Tei, S., & Alaerts, K. (2020). From thoughtless awareness to effortful cognition: alpha-theta cross-frequency dynamics in experienced meditators during meditation, rest and arithmetic. *Scientific Reports*, *10*(1), 5419.

47. Rodriguez-Larios, J., Wong, K. F., Lim, J., & Alaerts, K. (2020). Mindfulness training is associated with changes in alpha-theta cross-frequency dynamics during meditation. *Mindfulness*, *11*(12), 2695-2704.

48. Russell, J. A. (1980). A circumplex model of affect. *Journal of personality and social psychology*, *39*(6), 1161.

49. Samaha, J., Bauer, P., Cimaroli, S., & Postle, B. R. (2015). Top-down control of the phase of alpha-band oscillations as a mechanism

for temporal prediction. *Proceedings of the National Academy of Sciences*, *112*(27), 8439-8444.

50. Sauseng, P., Klimesch, W., Heise, K. F., Gruber, W. R., Holz, E., Karim, A. A., ... & Hummel, F. C. (2009). Brain oscillatory substrates of visual short-term memory capacity. *Current biology*, *19*(21), 1846-1852.

51. Seth, A. K. (2013). Interoceptive inference, emotion, and the embodied self. *Trends in cognitive sciences*, *17*(11), 565-573.

52. Shaffer, F., McCraty, R., & Zerr, C. L. (2014). A healthy heart is not a metronome: an integrative review of the heart's anatomy and heart rate variability. *Frontiers in psychology*, *5*, 1040.

53. Soriano, J. R., Rodriguez-Larios, J., Varon, C., Castellanos, N., & Alaerts, K. (2024). Brain–Heart Interactions in Novice Meditation Practitioners During Breath Focus and an Arithmetic Task. *Mindfulness*, *15*(9), 2218-2232.

54. Szymanski, C., Pesquita, A., Brennan, A. A., Perdikis, D., Enns, J. T., Brick, T. R., ... & Lindenberger, U. (2017). Teams on the same wavelength perform better: Inter-brain phase synchronization constitutes a neural substrate for social facilitation. *Neuroimage*, *152*, 425-436.

55. Thompson, E., & Varela, F. J. (2001). Radical embodiment: neural dynamics and consciousness. *Trends in cognitive sciences*, *5*(10), 418-425.

56. Tort, A. B., Kramer, M. A., Thorn, C., Gibson, D. J., Kubota, Y., Graybiel, A. M., & Kopell, N. J. (2008). Dynamic cross-frequency couplings of local field potential oscillations in rat striatum and hippocampus during performance of a T-maze task. *Proceedings of the National Academy of Sciences*, *105*(51), 20517-20522.

57. Valencia, A. L., & Froese, T. (2020). What binds us? Inter-brain neural synchronization and its implications for theories of human consciousness. *Neuroscience of consciousness*, *2020*(1), niaa010.

58. Vlemincx, E., Walentynowicz, M., Zamariola, G., Van Oudenhove, L., & Luminet, O. (2023). A novel self-report scale of interoception: the three-domain interoceptive sensations questionnaire (THISQ). *Psychology & Health*, *38*(9), 1234-1253.

59. Yakubov, B., Das, S., Zomorrodi, R., Blumberger, D. M., Enticott, P. G., Kirkovski, M., ... & Desarkar, P. (2022). Cross-frequency coupling in psychiatric disorders: a systematic review. *Neuroscience & Biobehavioral Reviews*, *138*, 104690.

60. Young, A., Hunt, T., & Ericson, M. (2022). The slowest shared resonance: a review of electromagnetic field oscillations between central and peripheral nervous systems. *Frontiers in Human Neuroscience*, *15*, 796455.

61. Young, A., Robbins, I., & Shelat, S. (2022). From micro to macro: The combination of consciousness. *Frontiers in Psychology*, *13*, 755465.

62. Young, A., Roberts, J., Baumgart, S., & Schooler, J. (2024, April 11). Cross-Frequency Coupling Between Brain and Body Rhythms as Modulated by Affect. https://doi.org/10.17605/OSF.IO/M85WP

63. Zelano, C., Jiang, H., Zhou, G., Arora, N., Schuele, S., Rosenow, J., & Gottfried, J. A. (2016). Nasal respiration entrains human limbic oscillations and modulates cognitive function. *Journal of Neuroscience*, *36*(49), 12448-12467.